11. A STUDY ON DAMAGE SCENARIOS FOR RESIDENTIAL BUILDINGS IN CATANIA CITY

(E. Faccioli, V. Pessina, G. M. Calvi and B. Borzi)

Abstract

The main purpose of this contribution is to illustrate the construction of damage scenarios for residential buildings in Catania city, both for a destructive earthquake (level I scenario event, M = 7) and a damaging earthquake (level II, M = 6.2), and to show the comparative performance of two alternative methods used for this purpose. The methods are representative of two different approaches to estimating the seismic vulnerability of structures, i.e. an empirical approach based on statistical score assignments (widely used in Italy and other countries) and a more recent, mechanical approach that uses displacement limit states associated with well-defined thresholds of structural damage. In the first part, we also compare the (actually used) deterministic evaluations of the scenario ground motions in the study area with probabilistic ones.

Different criteria for the representation of damage are applied and discussed. It is shown that the main scenarios obtained by the two methods are in reasonable agreement, provided a suitable percentile level for damage is chosen in the statistical score assignment approach

Key-words: building inventory, damage distribution, displacement limit states, earthquake scenario, ground shaking maps, seismic vulnerability, masonry buildings, reinforced concrete buildings, vulnerability index.

11.1 Introduction, deterministic vs. probabilistic ground motion descriptions

Two problems are to some extent typical in the process of constructing earthquake damage scenarios for old cities located in high seismicity regions of the Mediterranean: one concerning earthquake generation, and the other related to the features of the building environment.

As regards earthquake generation, scenario events can only rarely be associated with some confidence to the rupture of well-identified faults; many destructive earthquakes of the past typically occurred on blind faults, or on offshore faults. As one can gather from Part I of this volume, Eastern Sicily and Catania - catastrophically hit by two M~7 earthquakes in 1169 and 1693 - are no exception. Like in other earthquake catastrophes in Southern Italy, e. g. Messina – Reggio Calabria 1908, the fault ruptures of the 1169 and 1693 events occurred in all likelihood offshore, relatively close (10-15 km shortest distance) to the urban area of Catania, as argued in sub-sect. 1.2. However, this interpretation is not uncontroversial, since different source interpretations are also compatible with the distribution of 1693 felt intensities, as discussed in sub-sect. 1.3.

It has been argued that when the source location is uncertain, a probability-based description of the scenario earthquake is preferable to a deterministic one (see e. g. McGuire, 1995). However, when the scenario area lies in the near field of a

seismic source that may reach some tens of km in size, one can expect first-order rupture effects on ground motion that are difficult to treat in probabilistic hazard analyses. The same may happen in the presence of contrasted and irregular surface geology, likely to give rise to complex site effects. Catania is both close to the source of potentially large earthquakes and characterised by complex surface geology (see e. g. the geotechnical zonation in sub-sect. 2.2) and, hence, deterministic descriptions of the ground shaking were preferred in the Catania project.

Based on the historical seismicity and the seismo-tectonic context, and also on the needs of emergency planning by the Catania municipal administration, two different scenario events were assumed: a catastrophic earthquake (I_{MCS} = X) such as that devastating the city in 1693 and a damaging earthquake (I_{MCS} = VII-VIII) such as that of 1818 (see sects. 1 and 8 for location and more detailed characteristics). The GIS-based approach used to obtain the deterministic ground shaking maps for the scenario earthquakes, both in terms of peak acceleration and response spectral ordinates, is illustrated in sect. 3

To cast light on the possibility that a probabilistic format for the scenario ground motion may be unconservative for earthquake loss evaluations, we performed a probabilistic hazard analysis (PHA) using both the seismogenic zones of the well-known GNDT model, and the fault-like source-zone representing the segment of the Ibleo-Maltese fault, or Malta escarpment, assumed to have ruptured in 1693. For both geometric source models, shown in Figure 11.1, we computed by the Cornell's (1968) method the so-called «uniform risk» response spectra on soft soil and rock (lava flows) in Catania for 476 years recurrence period.

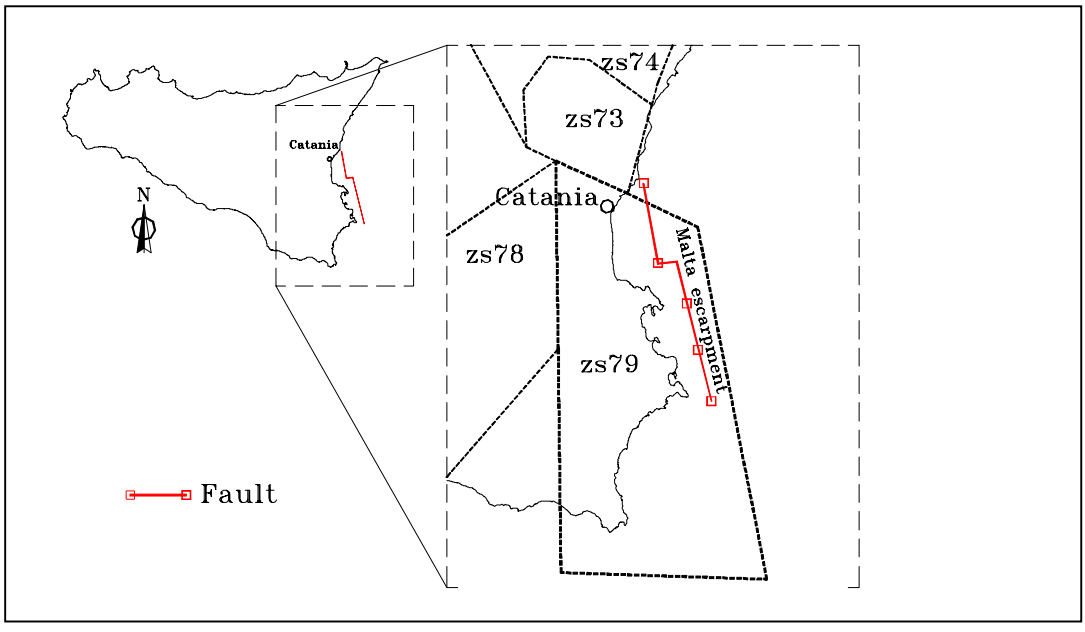

Fig. 11.1 - Seismic source models used for the probabilistic hazard analysis in Catania. Extended sources (78, 79,...) are from GNDT model (http://emidius.itim.mi.cnr.it/GNDT).

The background for the attenuation relation used (Ambraseys et al., 1996) is given in sect. 3. As illustrated in Figure 11.2, the 50-percentile probabilistic spectra for the fault source are about two-thirds the mean spectra computed deterministically for the assumed magnitude 7.3, with the same source geometry and attenuation relation. The consistent differences resulting in the spectra both at the 50-percentile and at the 81.4 percentile levels, due to the different representation of the seismogenic structures and their activity, is probably typical, and can provide guidance on the approach to be used in the choice of the scenario earthquake.

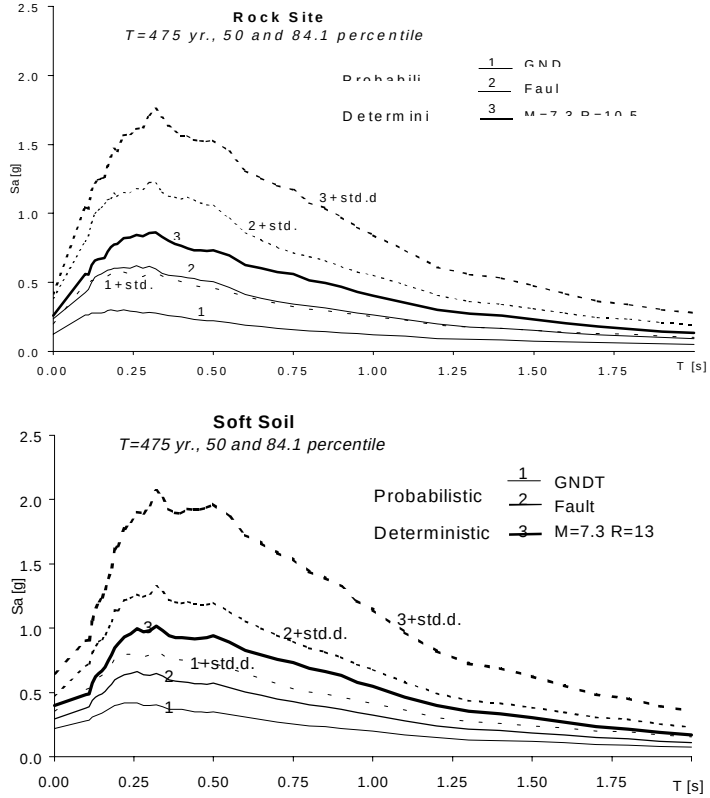

Fig. 11.2 - Comparison between the «uniform risk» spectra on rock and soil in Catania and the deterministic spectra.

While the basic description of the ground motion adopted in the project was deterministic, statistical distributions of the vulnerability and damage were necessarily adopted in the following steps of the scenario creation, as explained below.

Sect. 4 of this volume profusely illustrates how source and wave propagation modelling of acceleration synthetics in 2D and 3D was performed in the project. The synthetic ground motions, or quantities derived thereof, have been applied in the seismic response analysis of specific building and bridge structures in Catania, as shown in the other sects. of Part 4, while comparisons with the results provided by the empirical approach are given in sub-sect. 4.1 and sect. 3.

The second critical issue mentioned at the beginning concerns the difficulty of classifying a significant portion of the built environment (typically the oldest/weakest one) by well defined structural categories and construction periods. Unrecorded post-earthquake repairs, additions and modifications intervened in the course of centuries are not uncommon, and make it very difficult to characterise many building units (or building aggregates) in terms useful for large-scale vulnerability assessment and damage estimation. These issues are extensively treated in different parts of this volume, but most notably in sect. 5 concerning the assemblage of a general building database, and in sect. 9 for more specific aspects related to the masonry building stock

The age-class distribution of the prevailing structural types in Catania is illustrated in simplified terms in Figure 11.3, which depicts the growth of the urbanised area over three centuries; the significance of the periods in the legend will be clarified in the sequel. The post-1946 expansion of the city, in particular, is portrayed by the diffusion of the reinforced concrete (RC) buildings, typically up to 8-9 stories in height. It is instructive to compare Figure 11.3 with the density distribution of the population (1991 ISTAT census data) shown in Figure 11.4. The post–war growth was accompanied by an increase in population from some 250.000 inhabitants at the end of the war to a peak of 400.000 in 1971; the figure reported in the latest (1991) population census for the Catania municipality is 333.000 inhabitants in about 110.000 families. However, the present urban area extends well beyond the municipal boundaries and its population exceeds 500.000.

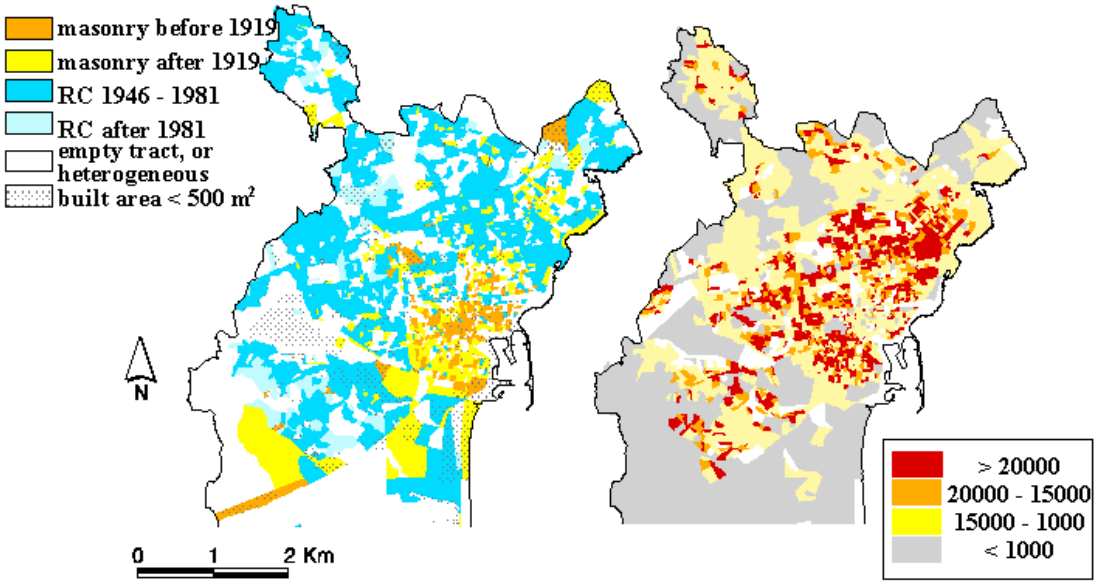

Figure 11.3 - Age class distribution of residential masonry and reinforced concrete (RC) buildings in Catania city, based on 1991 census data.

Figure 11.4 - Population density distribution (inhabitants/km^2) in Catania city.

Unlike other recent scenario studies of European cities, which are restricted to a part of the historic centre as in e.g. Lisbon (see D'Ayala et al., 1997), the basic choice made in this project was that the damage scenario should encompass the whole city (within the municipal boundaries).

The flow chart of Figure 11.5 outlines the essential components of the methodology adopted in this study. It is less comprehensive than, for instance, the approach incorporated in the software package HAZUS used in the U. S, (Whitman et al., 1997), because only the "direct damage" was considered and induced damage and indirect losses were neglected. This is because it is felt that in case of a repetition of the 1693 earthquake, the impact of direct damage in Catania would be dominant in terms of life and direct economic losses. For the level II scenario the situation could be some what different, but the expected impact is vastly inferior. On the other hand, induced damage is considered to be of limited importance, because liquefaction and slope failure hazards may occur only in limited zones outside the densely populated city area (see e. g. sub-sects. 2.5 – 2.6).

The most substantial part of our contribution consists of testing the applicability of different approaches to large-scale seismic damage evaluation, since we feel that comparative assessments of alternative damage prediction methods, that also require different ground shaking descriptions, are essential if earthquake scenario tools are to be applied with some confidence in a given country. Such assessments are unfortunately missing from practically all the recent earthquake scenario studies, and constitute one of the main motivations of this work.

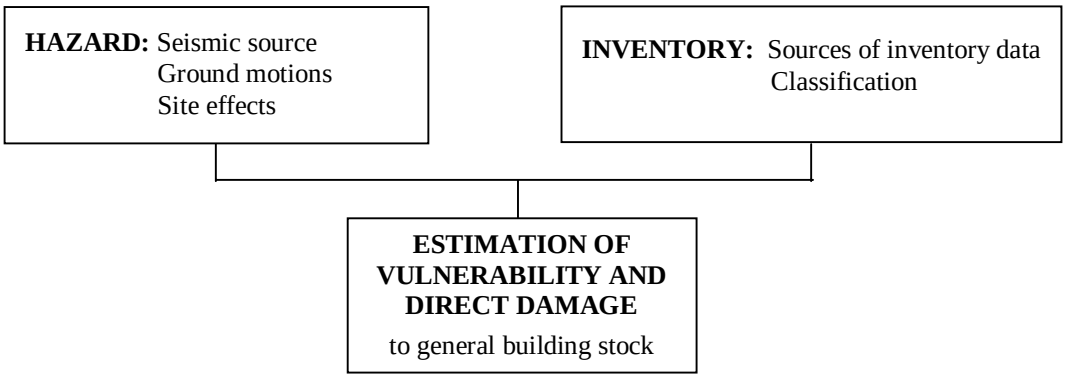

Figure 11.5 - Flow chart of the general methodology followed in this study.

The features of the two different approaches used for vulnerability assessment and damage estimation are first outlined in the following: one makes use of a statistical method based on standard score attributions (so-called GNDT method), and the other is derived from a mechanistic approach based on displacement limit states. Finally, different map representations of the damage distributions are illustrated and discussed for the Catania city area, for both of the assumed scenario earthquakes.

The vast amount of building inventory data, as well as the complexity of the physical environment data, made the use of a Geographical Information System (ArcInfo) virtually mandatory for this study. Furthermore, the GIS-generated damage distribution maps have also the advantage of being easily understood and used by city planners and risk managers.

11.2 Vulnerability assessment

A key feature of the Catania project is that a number of different methods were used for damage estimation, to allow for comparisons and to better gauge the extent of the uncertainties involved. Two such methods have been used in the present study, representative of two different approaches to estimating the seismic vulnerability of structures, i.e. an empirical approach based on statistical score assignments (widely used in Italy) and a more recent, mechanical approach that uses displacement limit states associated with well-defined thresholds of structural damage (Faccioli et al., 1999). Two additional approaches to vulnerability and damage evaluation are reported in another contribution in this volume (sub-sect. 9.5), namely the method of Damage Probability Matrices (DPM), and the VULNUS methodology, which makes use of fuzzy sets concepts and provides estimates of the failure probability of masonry buildings. These approaches have resulted – as one may check – in evaluations that are quite consistent with those reported herein as to the proportions of masonry buildings that are likely to suffer collapse or heavy damage. However, their application has not yet progressed to the point of providing damage distribution maps for the different sections of the city. Therefore, they will not be further discussed here.

11.2.1 *Assessment based on vulnerability score (GNDT method)*

Observation-based, statistical methods that assign a seismic vulnerability score to buildings are among the most widely used, see, e.g., ATC-21 (1988). To this category belongs also the approach that came to be known through the field version denominated «GNDT I and II level vulnerability forms» (Benedetti and Petrini, 1984; CNR-GNDT, 1994), widely applied in Italy, and also in some other European countries. A ‘rapid screening’ version of the same approach, has been specially devised for the LSU vulnerability survey of the Catania buildings, as documented in sect. 5 and in sub-sect. 9.5. This uses a single field-survey form that draws from both the level I and II forms. The vulnerability score is obtained from the weighted sum of the values of 11 parameters; however, only some of them are directly determined from the field survey (structural resisting system, non-structural elements, present state of building) or reasonably estimated from previous survey data and expert assessment, as in the case of the conventional shear resistance of masonry. The score for the remaining parameters (including, e.g., the configuration in plan and elevation) is assigned in a range of variation based on considerations on the historic or recent

construction practice in the city, and existing information from the national database. In this way a lower and upper bound value for the vulnerability index I_v (ranging between 0 and 100) has been assigned to each building. For the RC buildings in Catania, a re-calibration of the vulnerability model has been made using the data synthesised in DPMs for 1980 Irpinia (Southern Italy) earthquake (see Appendix).

The cumulative distributions of *Iv* derived from the LSU data by the rapid screening and score assignment procedures are shown in Fig. 11.6, both for the masonry and RC buildings.

For masonry, the I_v values based on the upper bound of the range mentioned above have been used. Inspection of the I_v statistical distributions and de-aggregation according to different indicators available from the ISTAT census, has led us – with some simplifications – to distinguish two age classes, i.e., buildings erected before and after 1919. The distinction is obviously crucial for the historic centre, where the pre-1919 buildings predominate and the correspondingly higher (by 10- to- 15 points) values of I_v strongly influence the predicted percentage of collapsed buildings. If the whole sample is considered and age classifications are neglected, the resulting cumulative distribution is very close to that for post-1919 buildings, since the sample size for the pre-1919 buildings is only a fraction of the total sample.

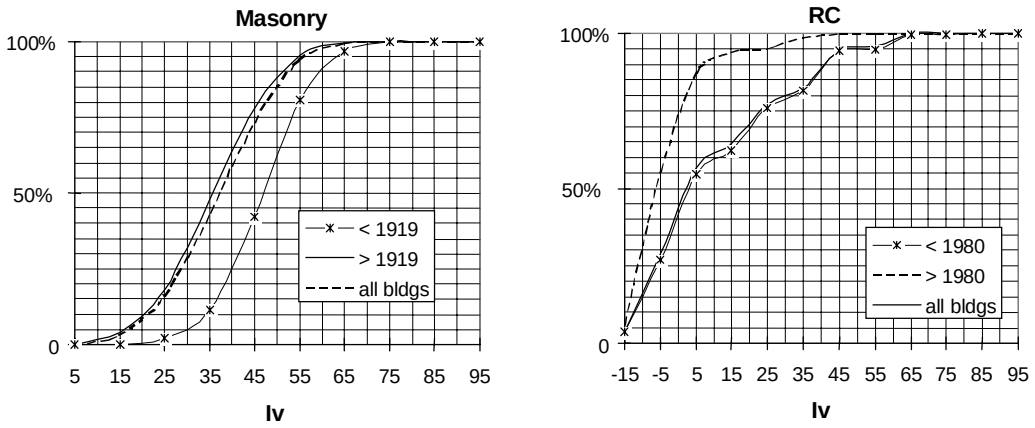

Figure 11.6 - Statistical distribution of the vulnerability index I_v for masonry and R.C. buildings base on the rapid screening data and procedure

For RC buildings, preliminary age classification analyses and the criteria used for developing the vulnerability model indicate that the year 1980 is necessarily the dividing line, because the enforcement of a seismic code started in 1981. Here, the sample size of the post-1980 RC buildings is 514 (updated as of January 1999). Thus, for RC buildings we also retain two separate vulnerability distributions based on the construction period, as shown in Fig. 11.6.

In conclusion, for damage evaluation within the score assignment approach, each residential building of the Catania inventory is characterised by one of the vulnerability distributions of Fig. 11.6, depending on age and type of resisting structure.

11.2.2 *Assessment based on displacement limit states*

An alternative method for evaluating the probability of attainment of a given limit state (LS), based on the assessment of the displacement capacity corresponding to the LS and of the displacement demand resulting from a displacement spectrum, has been applied (Calvi, 1999). The spectrum willl obviously depend on local site condition, but also on the dissipation capacity corresponding to LS and building type. In the worst case, the available data for a given building would include period of construction, number of stories and the basic construction material (i.e., concrete or masonry).

For RC buildings, the year of construction is used to detect whether some seismic provision was enforced at the time of construction. As a first criterion, buildings erected after 1981 (year of enforcement of seismic norms in the Catania municipality) have been classified as 'well designed', assuming a ductile response with a uniform distribution of energy dissipation capacity. For older buildings a limited ductility capacity, with a high potential for damage concentration (i.e. a soft-story type of response) or for fragile failure modes (e.g., shear failure modes), has been assumed. This assumption is perfectly consistent with the evidence and results of the analyses given in sect. 10.

In the displacement limit state approach, the following five post-earthquake situations of a building are assumed to be of interest for damage scenarios:

1. Essentially undamaged;
2. Slightly damaged, but usable without any repair or strengthening;
3. Extensively damaged, but still repairable
4. Not collapsed, but so severely damaged that it must be demolished;
5. Collapsed.

To assess these five possibilities four limit states have been defined, considering both structural and non-structural damage; the former is obviously fundamental to assess a probability of collapse, but the latter can govern in most other cases. In the present approach only inter-story drift has been considered. In several cases it is not reasonable to make distinctions between the first two or between the last two situations above, and the classes can be reduced to four or three. Keeping in mind that the results will have a statistical meaning, and that consideration of a single building may be completely misleading, the limit states are defined as follows:

LS1 Below this LS no damage, either structural or non-structural should take place and the expected response is essentially linear elastic.

LS2 Below this LS only minor structural damage and/or moderate non-structural damage can be accepted. The building is ready for occupancy after the earthquake, without any need for significant strengthening and repair to structural elements. Member flexural strengths could be attained, and some limited ductility developed. For masonry buildings a drift limit of 0.3% has been

considered appropriate, because of the increased structural damage at the same drift level.

LS3 Below this LS significant structural damage and extensive non-structural damage can be accepted. The building cannot be used after the earthquake without significant repair of the structure. Still, repair and strengthening is feasible. Fracture of transverse reinforcement or buckling of longitudinal reinforcement should not occur, and the core concrete in plastic hinge regions should not need replacement. An average drift limit between 0.5 and 1.5 % has been considered appropriate. Similar to the previous LS, a drift limit of 0.5% is set for masonry buildings.

LS4 Below this LS any level of damage can be accepted, provided that the building did not collapse. Repairing may be neither possible nor economically reasonable. The structure will have to be demolished after the earthquake. Beyond this LS global collapse with danger for human life has to be expected. Attainment of shear capacity or instability due to excess of displacement are examples of this LS.

The choice of the drift limit values is discussed by Calvi (1999). The method requires the definition of a structure-equivalent model for each LS and for each type of structure considered. Each model is defined in terms of secant stiffness to the maximum displacement allowed by the appropriate LS, and of a displacement demand reduction factor dependent on the energy dissipated by the structure, again for the appropriate LS. The paucity of the data used to define the equivalent model obviously results in a low reliability of estimate of the two parameters of the model. Therefore, intervals rather than single values will be defined for stiffness and damping. Within the surface obtained by the intersection of the two intervals, a uniform probability density function is assumed to assess the probability that the couple of parameters which represent most appropriately the actual response of the structure falls within a given sub-domain.

Possible out-of-plane failure modes are not considered in this approach. However, the expulsion of masonry walls may be a concern only for a class of buildings, which constitute roughly 7% of the masonry buildings total. We remind that for «building A» analysed in detail in sub-sect. 9.4 as representative of this class, overturning is found to occur for the 0.35 g peak acceleration; however, the phenomenon is prevented by elimination of horizontal thrusts at the upper stories.

In order to define the limit displacements and equivalent period of vibration, the dimensions of vertical structural elements must be known. Data from both the ISTAT and LSU datasets were considered. For the ISTAT data set, which includes all residential buildings in the city but does not provide the dimensions of structural elements, the column size in RC buildings was assumed vary in the range 0.3 to 0.5 m and the inter-story height, both for RC and masonry buildings, between 3 m and 4.5 m. On the other hand, the LSU data set, provides more detailed information on the structural elements and the characteristics of the structural system.

The results obtained from ISTAT and LSU data were reasonably close, with the exception of the LS3 limit state for well designed RC buildings, which is negligible in terms of number of cases. It was therefore deemed acceptable to examine the results from the ISTAT dataset, which covers the whole urban area. Based on the analyses performed, two representative vibration periods for masonry and RC buildings have been identified, namely:

- 0.4 s, characteristic period of vibration of masonry buildings for the severe damage limit state (LS4), that has a high probability of being attained, and
- 1 s, median period of RC buildings considering non structural damage that is the dominant condition for this kind of structures.

Needless to say, these are the values of the vibration period for which ground motion maps in terms of displacement spectral response (at appropriate levels of damping) were generated.

11.3 From ground shaking and vulnerability to building damage

In the process of obtaining the damage estimations, we have assumed in the first step that the scenario ground shaking is deterministically given. Next, to cope with the large uncertainties at play, the relevant structural characteristics of buildings have been characterised as random variables. This is done through empirical distributions for the vulnerability index I_v, as in the GNDT approach, or making use of uniform probability density over appropriate intervals of the governing structural, as in the LS approach. The latter intervals define a domain of spectral response vs. period that, when compared with the seismic demand (displacement spectrum of scenario earthquake), allows to directly estimate the probability that the actual response of the structure leads to a given post-earthquake damage state for a building.

To link vulnerability and level of ground shaking to building damage in the score assignment approach, a deterministic correlation with the characteristics shown in Fig. 11.7 has been assumed. This was calibrated on damage observations from the 1976 Friuli and 1984 Abruzzo earthquakes; although it is affected by considerable dispersion, it has been extensively used in Italy in recent years.

The damage factor d, i. e. the ratio between the repair cost and the replacement cost of a building, is used as a damage indicator in Fig. 11.7 and in the following; d is assumed to vanish for peak ground acceleration values less than a threshold y_i, and to increase linearly between y_i and a collapse acceleration y_c. Each of the curves in Fig. 11.7 corresponds to a different vulnerability index.

Concerning the reliability of the limiting accelerations values appearing in Fig. 11.7, the detailed non-linear analyses performed on the pre-1981 RC Monterosso building in Catania (sect. 10), with beams spanning in one direction only, have yielded accelerations for initiation of damage of 0.03-0.05g. while the largest value determined for the base shear coefficient is about 0.13g (in the weakest direction) for a model including well-executed infill walls.

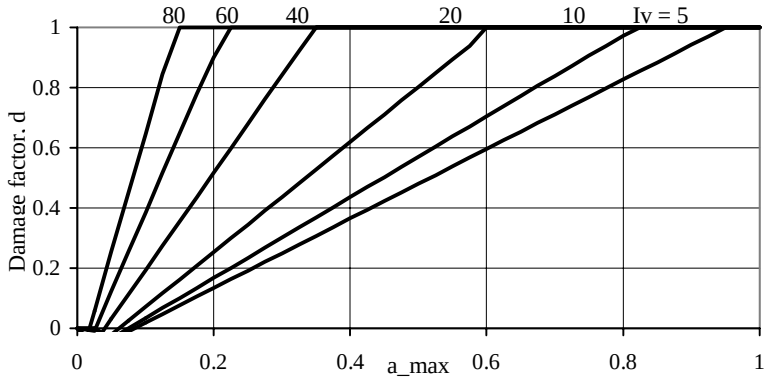

Figure 11.7 - Vulnerability-damage-peak ground acceleration relationship for masonry and R.C. buildings. Shown on the curves are some values of the vulnerability index (from CNR-GNDT, 1993).

A different, independent vulnerability and general damage evaluation has also been carried out on the basis of a carefully selected sample of 135 masonry buildings in Catania using the so-called VULNUS methodology, and Damage Probability Matrices calibrated on the 1980 Irpinia earthquake (see sub-sect. 9.5). With a reference PGA of 0.30g over much of the city area for the level I scenario earthquake (see ground motion maps in sub-sect. 3), this alternative approach leads to probabilities of very heavy damage or collapse in the range between 0.60 and 0.90 for the entire sample of 135 buildings. For areas with PGA around 0.20g, the same probability is in the 0.25-0.70 range. These estimates are basically consistent with the results obtained in this study. However, the broadness of the indicated ranges suggests that considerable caution should be exercised in predicting the damage scenarios for masonry buildings under the assumed reference events.

As is often the case with damage scenarios, we chose to represent damage at the census tract level. To evaluate the damage factor in each tract, we used for the ground motion parameter (PGA or displacement spectral ordinate) the value at the tract centre of gravity; where an abrupt change in site conditions would occur inside the tract, such as those arising from contacts between lava flows and a clay unit, the highest ground motion value was used.

Within the statistical approach, starting from the I_v distributions of Fig. 11.6 and the applicable PGA values, four different damage distributions were generated for each census tract. At this stage, different criteria can be followed to obtain a single, synthetic indicator of damage for the tract. One option is to sum, for an assumed probability level (or percentile), the values of the damage factor yielded by the individual distributions, weighted in proportion to the number of buildings present in the tract for the corresponding age class and structural type. Alternatively, the damage in the tract (for the assumed percentile level) can be represented by means of the prevailing value range of *d*, i.e., the range affecting the category with the largest number of buildings present in the tract; hence, in this case, no weighting is performed. The damage scenario corresponding to the latter option is illustrated in

Fig. 11.8 (map on left-hand side) at the 50-percentile level; the elementary cell in the maps is the ISTAT census tract. Although this scenario does not drastically differ from that based on the weighted damage for the same percentile, illustrated in Fig. 11.9b, a stronger incidence of zones with high damage can be noted in the former (Fig. 11.8, left) in the historic city centre and surroundings. This is because the prevailing damage is here governed by the older, more vulnerable masonry buildings. On the other hand, in several sections to the N and E of the centre, the prevailing damage (Fig. 11.8, left) is less than the weighted one (Fig. 11.9b) since RC construction is predominant.

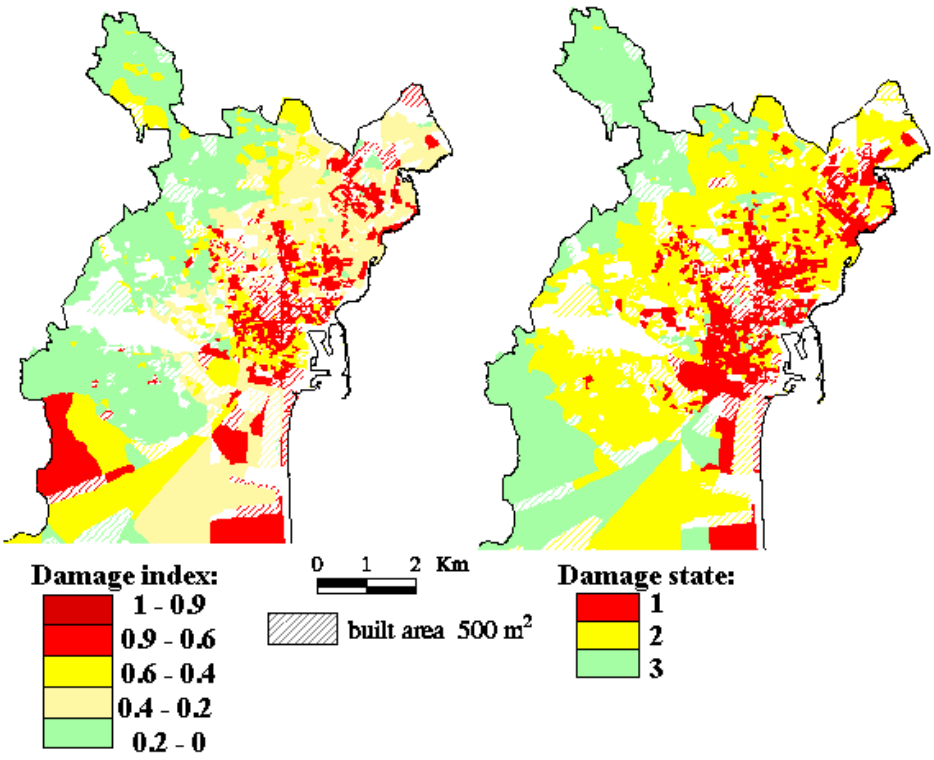

Figure 11.8 - Maps of predicted damage to residential buildings for the level I scenario earthquake, based on the prevailing damage in each census tract. Left, predicted by the statistical score assignment (GNDT) approach at the 50-percentile level; right, predicted by the displacement limit state approach

The choice of the percentile level for the damage representation should be considered in the light of the different requirements arising from the perspectives of emergency management and risk reduction policies. Thus, the 50-percentile representation may be better suited for estimating the overall urban area affected by light ($d < 0.2$ and buildings available for immediate occupancy after the earthquake)

and intermediate levels of damage (*d* up to, say, 0.6, and buildings not suitable for immediate occupancy). As such, it could be used for estimating the number of people to be sheltered in the emergency phase, as well as to obtain a rough, order-of-magnitude estimate of the costs of strengthening and upgrading a large part of the existing building stock. On the other hand, a scenario at the 90-percentile level – not shown here – would be suitable for upper bound estimates of the extent of severely damaged or collapsed buildings (indicatively, $d > 0.9$) and, hence, of the number of victims.

The damage predictions obtained from the displacement LS approach have shown that the limits imposed by non-structural damage are in most cases dominating for RC buildings. Actually, the large majority of RC buildings are found to fall into the 'extensively damaged, still repairable' class, due to the influence of non-structural damage. It can be observed that a dominant period of vibration around 1 s was found for this case. For masonry buildings the case of «severely damaged, not repairable» buildings is dominating, with a significant portion of buildings predicted to collapse when the number of stories tends to increase. Considering all RC and masonry buildings together, the LS yields a prediction of extensive damage, more or less repairable, for approximately 60 % of the total building stock.

The spatial distribution of damage from the LS approach is also depicted in Fig. 11.8 (map on right-hand side), allowing an interesting comparison of the two approaches adopted. Although the damage scales in the two maps are intrinsically different, if the prevailing damage class is considered for each census tract (as in the figure), a remarkable similarity of damage distribution and intensity is evident. In the map obtained by the GNDT approach, the highest risk zones include the oldest city sections (historic centre and surroundings, adjacent to the harbour) with the expected high incidence of collapse/heavy damage cases of masonry buildings, and also some sections to the NE, with heterogeneous presence of both masonry and the weaker, pre-1981 RC constructions. The high damage predicted in the NE parts of the municipality corresponds to the areas with the strongest ground shaking. The relative arbitrariness involved in choosing a 50-percentile level for the left-hand map in Fig. 11.8, and in assuming a correspondence between damage factor and predicted damage state can probably explain the somewhat larger extension of higher damage shown on the right-hand map of Fig. 11.8.

Finally, we illustrate the damage distribution for the level II scenario (repetition of the 1818 earthquake), obtained with the GNDT approach, 50-percentile level, and weighted damage representation. The resulting map is shown in Fig. 11.9, side by side with the corresponding map for the level I event. To grasp the differences in the two damage scenarios, it is essential to remind (see sub-sect. 1.2 and sect. 3) that, in addition to a difference of about one magnitude unit, the source assumed for the level II event is fairly close to the northern sectors of the municipal area. Hence, not only is the level II damage intensity consistently inferior to that of level I, but it also exhibits a different spatial pattern, rapidly decreasing with distance from N to S. Therefore, even in relative terms, we do not see in Fig. 11.9 a) any significant concentration of damage in the older city sections. Also, the incidence of

site amplification, which controls the location of some high damage spots in the level I scenarios, plays now a less prominent role. By and large, the damage scenario for an earthquake like that occurring in 1818, shows that a large part of the city can expect a non-negligible level of damage, but very little, if any, destructive damage and victims.

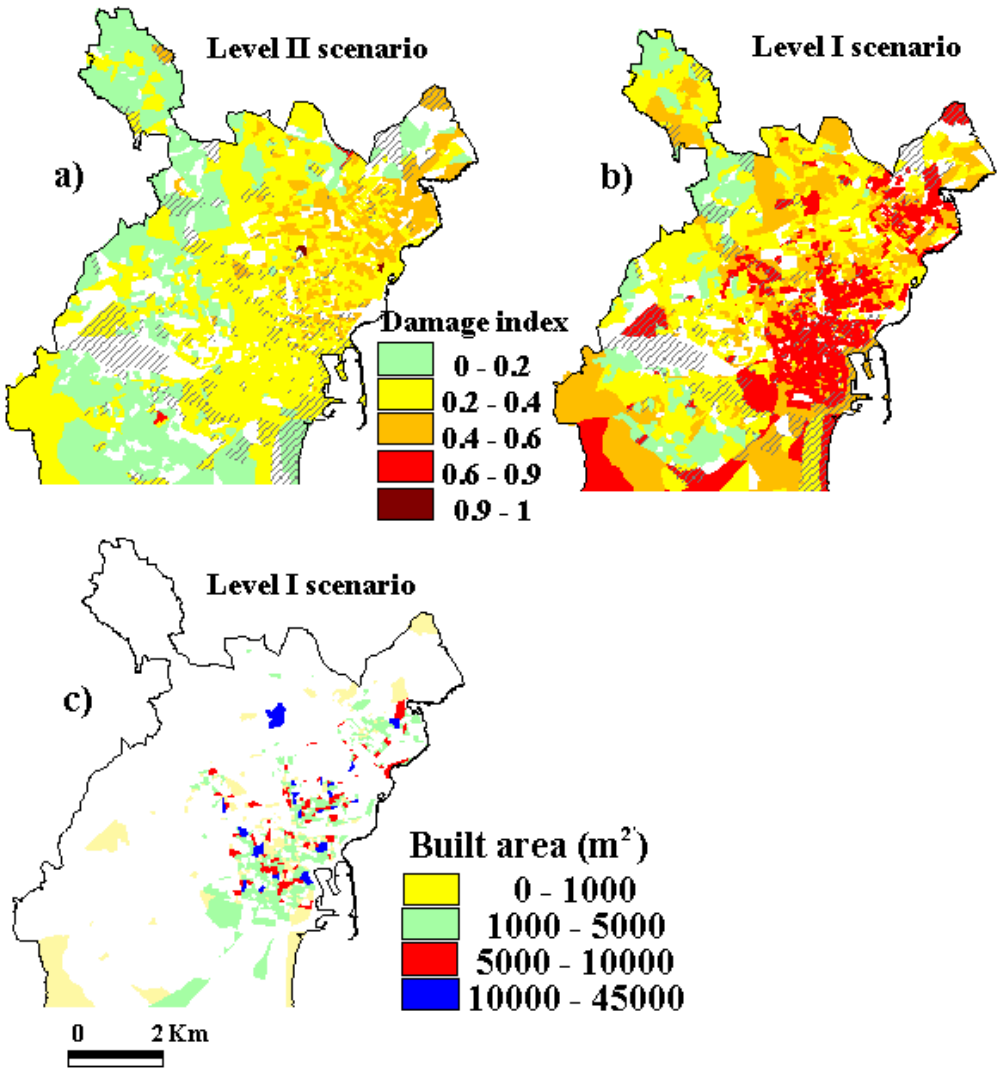

Fig. 11.9 - Maps of predicted damage to residential buildings, based on the GNDT approach at the 50-percentile level, weighted damage, for: (a) level II scenario (1818 earthquake) and (b) level I scenario (1693 earthquake). (c) map showing the level I scenario distribution of the built area (in m^2), in each census tract, suffering heavy damage or collapse.

Scenario maps representing the distribution of a damage index, or a damage state, as in Figs. 11.8 and 11.9 (a, b), may not be an optimal tool for local administrators and emergency planners, who could need a more quantitative assessment of the impact of a potentially destructive earthquake. One option is to represent in each city block (or census tract, as here) the amount of built area affected by heavy damage or collapse, i. e. predicted to require almost surely post-event demolition. If we choose $d > 0.6$ as a significant threshold for heavy damage, we obtain for the level I scenario the distribution map of Fig. 11.9c, which can be usefully compared also with the population density map in Fig. 11.4. One may note that a representation such as that of Fig. 11.9c probably provides a more realistic picture of the destructive earthquake impact. The corresponding map for the level II scenario is not shown, because it is empty.

11.4 Conclusions

The study illustrated herein presents, to our knowledge, the first attempt at constructing a complete damage scenario of residential buildings for both a potentially catastrophic and a damaging earthquake in a mid-size European city. Emphasis has been laid on some methodological aspects, that have sometimes been overlooked in recent literature on seismic damage scenarios. As a first indication, the need to use engineering ground motion parameters such as peak acceleration or response spectral ordinates as quantitative indicators of ground shaking is stressed. Such parameters can, in fact, appropriately and easily account (through the use of recent attenuation relationships) for the often dominating influence of site effects, and of near-field conditions, when the source of large earthquakes is close to the area of study. This also implies, especially for European countries, that vulnerability-damage models should be as much as possible updated in terms of engineering ground motion parameters, rather than of macroseismic intensity. The use of synthetics generated by different source representation and wave propagation algorithms, while strongly recommended for generating the input of parametric response analyses to specific structures, cannot yet be used with the same level of confidence as the simpler engineering approach based on attenuation relations.

The second key issue addressed in this paper has to do with the difficulties involved in constructing a reliable and fit-for-the-purpose inventory of existing buildings. While we believe that Catania may be better off than many European cities from the viewpoint of available information that describe the built environment, it is evident that an inventory suitable for seismic evaluations requires substantial effort in terms of using, interpreting, and adapting different sources of data. In fact, for cities characterised by high vulnerability and seismic hazard, specific rapid-screening surveys of the type described here are probably indispensable. For these reasons, statements of the type ‘building inventory data were assembled from the tax assessor’s file’ or the like, sometimes encountered in the

current literature on the subject (especially in the U.S.), should be regarded with skepticism.

For a comparative evaluation of the results obtained, we have used two alternative methods to predict damage scenarios for residential buildings. The first one (GNDT approach) belongs to the family of the score assignment, statistical methods and is in many ways comparable to the ATC-13 method used in the U.S.; it has enjoyed considerable diffusion in Italy and in recent projects in other European countries, and has the advantage of being calibrated in part on damage statistics of recent Italian earthquakes. The second approach, based on the use of displacement limit states as indicators of post-earthquake damage situations, is a novel one and needs further field checks. However, it has the advantage that it can naturally account for the parameters controlling the dynamic response of buildings (fundamental period and dissipated energy), and was calibrated on large-scale laboratory tests at least for masonry structures. Thus, it is remarkable that the scenarios predicted through the two approaches are quite similar, although a detailed quantitative comparison is made difficult by the intrinsic differences in the two methods.

A further point regards the criteria used for damage representation: while the prevailing and weighted (over the census tract) damage criteria lead to compatible results with clearly interpretable differences, the choice of the percentile level to be used for the prediction should be tailored to the requirements of city planners and risk managers, and the need of documented case histories is clearly felt. Finally, scenario maps showing the absolute values of built area (in each census tract) predicted to suffer heavy damage or collapse are likely to provide a more realistic picture of the destructive impact of a strong earthquake.

Acnowledgments

We acknowledge the cooperation by Alessandro Rasulo who performed the probabilistic hazard analyses illustrated in Figures 11.2 and 11.3. This work has been supported by Italy's National Research Council (CNR) under Research Contributions 97.00513.PF54 and 98.03203.PF54.

References

Ambraseys N.N., Simpson K.A., Bommer J.J. (1996). Prediction of horizontal response spectra in Europe, *Earthquake Engineering and Soil Dynamics*, 25, 371-400

ATC-21 (1988). Rapid visual screening of buildings for potential seismic hazard,: a handbook, Applied Technology Council, Redwood City, California

Benedetti D., Petrini V. (1984). On seismic vulnerability of masonry buildings: proposal of an evaluation procedure, *L'industria delle Costruzioni*; volume **18**, pp. 66-78 (in Italian).

Calvi G.M. (1999). A displacement-base approach for vulnerability evaluation of classes of buildings, *J. Earthquake Engineering*, Vol. **3**, N. 3, 411-438.

CNR - GNDT (1993). Esismic risck for public buildings, PArt I, Methodological aspects, Gruppo Nazionale per la Difesa dai Terremoti - Roma (in Italian).

CNR - GNDT (1994). *Exposition and 1st level vulnerability and damage survey form*, Gruppo Nazionale per la Difesa dai Terremoti - Roma (in Italian).

Cornell C. A. (1968). Engineering seismic risk analysis, *BSSA*, vol **58**, pp.1583-1606.

D'Ayala D., Spence R., Oliveira R., Pomonis A. (1997). Earthquake loss estimation for Europe's historic town centers, *Earthquake Spectra*, Vol. **3**, N.4, pp.773-793

Faccioli E., Pessina V., Calvi G.M., Borzi B. (1999). A study on damage scenario for residential buildings in Catania city, *J. of Seismology*, Vol.**3**, N. 3, 327-343

McGuire R. (1995). Scenario earthquakes for loss studies based on risk analysis, *Proc. Intern. Conf. on SeismicZonation*, Nice, Oct. 17-19, Vol. **II**, 1325-1333.

Whitman R.V., Anagnos T., Kircher C.A., Lagorio H.J., Lawson R.S., Schneider P., (1997). Development of a national earthquake loss estimation methodology, *Earthquake Spectra* **13** (4), pp. 643–661.